Simulation of Energy Recovery from Chimney Hot Gases Using an Encapsulated Phase Change Materials Heat Exchanger

Ehsan Mehrabi Gohari[1,*], and Moslem Mohammadi Soleymani[2]

[1] *Department of Mechanical Engineering, National University of Skills, Tehran, Iran*
[2] *Department of Mechanical Engineering, Payame Noor University, Tehran, Iran*
**Corresponding author: e.mehrabi@pnu.ac.ir*

Manuscript received 19 July, 2024; revised 26 September, 2024; accepted 18 November, 2024. Paper no. JEMT-2407-1520.

The present study concentrated on devising a novel heat exchanger that employs materials that undergo phase transitions between solid and liquid states. In this context, air and water were selected as the fluids, while paraffin, potassium fluoride tetrahydrate, and potassium nitrate70%(Kno3-Lino3) were used as the phase change materials. The research scrutinized twelve distinct models in Axisymmetric two-dimensional and transient modes. Additionally, the proposed model was employed to assess the impact of factors such as the porosity, diameter, and type of encapsulated phase change material, as well as the temperature and flow rate of the inlet fluid on the thermal performance of the model. The results indicate that the simulated heat exchanger possesses the potential to harness energy from hot exhaust gases. The investigation of the particle diameter and porosity revealed that decreasing the porosity and increasing the particle diameter enhanced the energy storage and overall performance of the heat exchanger. Furthermore, the examination of varying input temperature and flow rate demonstrated that raising the temperature of the chimney gases enhances the heat exchanger performance, while increasing the inlet fluid flow rate reduces the charging time. Notably, the study also found that using potassium nitrate70% increase the amount of stored energy compared to other mentioned materials, due to the improved properties and high melting temperature.

Keywords: *Encapsulated phase change materials, Thermal energy storage, Energy recovery, Latent heat.*

http://dx.doi.org/10.22109/jemt.2024.468628.1520

Nomenclature

ρ_s	Density of particle
D	Diameter of heat exchanger
H	Heat exchanger height
Th	Wall thickness
ρ_f	Density of fluid
$c_{p,s}$	Specific heat capacity of particle
$c_{p,f}$	Specific heat capacity of fluid
θ_s	Solid volume fraction
d_{pe}	Particle diameter
ϵ_p	Porosity
L	Latent heat
$\rho phase1$	density of the solid phase
$Cpphase1$	heat capacity of the solid phase
Kphase1	Conductive heat transfer coefficient of the solid phase
$\rho phase2$	density of the liquid phase
$Cpphase2$	heat capacity of the liquid phase
Kphase2	Conductive heat transfer coefficient of the liquid phase

1. Introduction

Considering the increasing global population and economic growth, the demand for energy is on the rise. As a result, scientists and engineers are seeking energy management methods and systems to boost productivity, control energy storage, curb unnecessary energy consumption, and reduce production costs across various industries. While renewable energy sources, such as solar and wind power, have garnered more attention, their unreliability has limited their widespread use. Heat recovery from hot gas currents in operational units, particularly in process units, can be considered as an alternative solution to decrease energy consumption. This approach ultimately leads to a reduction in energy consumption intensity [1-3].

In current industrial operations, a significant amount of high-temperature gas is generated through the combustion of fuel in boilers and various furnaces. It is crucial to explore opportunities for recycling this energy to minimize overall energy consumption within the same unit or other operational units. The thermal quality and quantity of generated heat play pivotal roles in justifying the economic viability of energy recycling initiatives. Typically, the output streams from high-temperature operational units are more economically sustainable for integrating recycling units owing to their favorable thermal characteristics. In a related study, Shahabi et al. studied the effect of using a heat recovery system in Semnan gas turbines in a Shahroud oil pumping station on energy saving. They showed that using a heat recovery turbine reduces the energy required for pumping [4]. The selection of suitable heat storage and steam production systems is contingent upon comprehensive economic evaluations and feasibility studies. Recent research has emphasized the importance of optimizing both tangible and hidden heat storage systems in terms of their structural and functional aspects. [5]. Several systems with various applications are available for heat recycling. The selection of an appropriate system for each process depends on various factors, such as gas temperature, operating system pressure, permissible pressure drops, type and characteristics of the functional fluid, and dimensional and structural constraints. Storage-type heat exchangers, also known as regenerators, are energy recovery systems in which two currents pass through the same path one after the other. These heat exchangers have an uncommon arrangement for the flow of currents, including opposite, parallel, and cross flows. In a storage-type heat exchanger, both fluids pass through the same path, thereby facilitating heat transfer. During the operation of a regenerator, heat energy is transferred from the hot fluid to the bed and is stored in the bed when the hot fluid flows over the heat transfer surface. As the cold fluid passed through the same bed, heat energy was released from the bed and transferred to the cold fluid. In this manner, the heat energy is periodically stored in the bed and then released. To ensure the continuous operation of the regenerator within the appropriate temperature range, the fluids, valves, and bed were changed in cycles, providing the same level of heat transfer for the cold and hot fluids. The periods during which the warm fluid flows through the cold bed and the cold fluid passes through the hot bed are known as heating and cooling periods, respectively. It is not necessary for these periods to be equal to achieve efficient operation. After changing the flow from hot to cold or vice versa, a small amount of fluid may become trapped inside the exchanger, which is unavoidable [6]. Energy storage refers to the accumulation of energy when energy is present and its exploitation when it is absent, which creates a balance between production and energy consumption. Electrical, mechanical, and thermal energy storage are the most important methods of energy storage [7]. Researchers have investigated the use of phase change materials to enhance the efficiency of thermal energy storage systems. Sinka et al [8] conducted experiments to evaluate phase change materials in hot summer conditions, aiming to utilize lightweight materials with suitable thermal mass to lower internal temperatures. Their findings demonstrated that integrating phase change materials into the roofs of buildings led to a decrease in the room air temperature by 0–2 °C. In a related study, Parviz et al. [9] explored the combined impact of condensers and phase change materials on the performance of a single-slope solar water softener using experimental methods. The results revealed a 17% increase in the daily productivity of the proposed desalination plant compared with traditional desalination methods. Additionally, Ebadati et al. [10] examined the effect of phase change materials in building shells on the energy consumption storage. Their simulation results indicated a notable reduction in heat transfer when utilizing phase change materials in building shells, resulting in a decrease in the annual energy consumption of up to 3.97%. This study employed the latent heat method for thermal energy storage. This system utilizes phase change materials to store energy. These materials have the capacity to absorb and retain latent heat energy, allowing thermal energy storage during the phase change process. Notably, the phase change material could retain this latent heat energy across numerous phase-change cycles without any deterioration. Compared with sensible heat storage materials, phase-change materials demonstrate a higher thermal energy storage density and can absorb or release substantial energy at a consistent temperature [11]. Oudaoui et al.[12] studied thermal behavior of a solar heat exchanger using multiple phase change materials and they showed that the design and the optimization of solar energy systems by using phase change materials, leading to more sustainable and efficient utilization of renewable energy resources. When storing thermal energy through phase change, the materials used should possess high latent heat and high thermal conductivity based on their intended application. The physical and chemical properties of these materials play a crucial role in the design of heat-recycling systems. Phase-change materials are classified according to their melting temperature and composition. Melting temperature ranges are divided into two main groups: low-temperature (below 200 °C) and high-temperature (above 200°C). Furthermore, composition-based classification includes organic, inorganic, and eutectic compounds [5].

In today's industry, the majority of phase change materials have low thermal conductivity coefficients. Consequently, this leads to decreased efficiency in certain thermal energy storage systems, making it challenging to justify such systems economically. Various methods have been utilized to enhance the efficiency of these energy storage systems. These approaches include encapsulating phase change materials, employing multiple phase change materials, boosting their thermal conductivity of phase change materials, adding different weight percentages of various nanoparticles in standard phase change materials and utilizing expanded surfaces (fin installation) [13-23].

In this research, a new heat exchanger structure, including an encapsulated phase change material, is proposed to recover energy from hot exhaust gases. Hot gases were selected as the heating fluid; water as the cooling fluid; and paraffin, potassium fluoride tetrahydrate, and potassium nitrate 70% (Kno3-Lino3) were selected as phase change materials. Investigations have been conducted for different models in axisymmetric two-dimensional and unsteady modes, and using the developed model, the effects of porosity, diameter, and type of phase change material, as well as the temperature and flow rate of the inlet fluid on the thermal performance of the proposed model were investigated.

2. Methodology

Considering the significance of conserving energy and the substantial thermal energy storage capacity of phase change materials, we conducted a study to develop a novel exchanger design incorporating encapsulated phase change materials. The goal was to capture energy from hot waste gases in factories. We used different geometries of the heat exchangers and different materials that changed from solid to liquid. The schematic of the simulated heat exchanger is illustrated in Figure 1, and detailed model specifications are provided in Table 1. During the modeling phase, we utilized hot air as the heating period fluid and water as the cooling period fluid, considering that exhaust gases primarily contain nitrogen, oxygen, and carbon dioxide. Our investigations involved varying the inlet temperature and the mass flux. Table 2 lists the thermophysical properties of the hot air and water used. In addition, we explored the impact of encapsulated phase change materials on the thermal performance of modern heat exchanger. Three distinct types of phase change materials were employed, and their thermophysical properties are listed in Table 2.

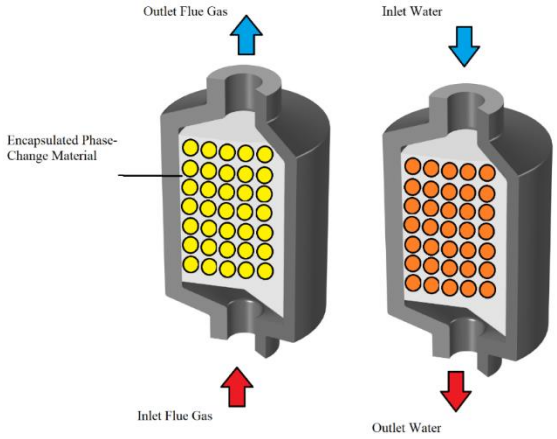

Fig.1. Schematic of the studied heat exchanger.

Table 1. Geometric specifications of the studied models[24,25].

Geometry details	Size
D	36 cm
H	47 cm
d_{pe}	1-10 mm
Th	5 cm
ϵ_p	0.2-0.9

Table 2. Thermophysical properties of materials used

Type of material	ρ (m^3/kg) Solid-liquid	CP (J/kg°C) Solid-liquid	L_f (kJ/kg)	Melting point (°C)	K (W/m°C) Solid-liquid
Paraffin	778-861	1850-2380	213	60	0.4-0.015
KNO_3-$LiNO_3$ 70-30%	1930	1626	155	124	0.58-0.58
KF.4H2O	1437-1435	1620 2480	231	18.5	0.62-0.486
Air	1.1644	1.0064	--	--	0.0264
Water	997.1	4179	--	100	0.613

2.1. Solution Method and Governing Equations

In this study, an Axisymmetric two-dimensional model in COMSOL 6.1 software is presented to compile and formulate the heat transfer and fluid flow in a heat exchanger containing encapsulated phase change materials. Using this model, the heat exchanger can be considered a homogeneous porous medium consisting of spherical capsules. In this model, the momentum and energy equations were solved according to the physics of the problem. The momentum equation is solved in a steady state, the energy equation is solved in a non-steady state, and in order to increase the accuracy of the calculations, the convergence accuracy of 10^{-12} is considered. Figure 2 shows the convergence diagram of velocity and pressure and turbulent flow variables for the simulation performed in steady mode and Fig.3 shows the convergence diagram of the non-steady solution, also the assumptions included to derive the equations are: 1- The thermophysical properties of solid and liquid phase change materials are assumed to be constant and are not dependent on temperature.2- During the PCM phase change process, the volume change of the phase change material is insignificant.3- The effect of natural convection in liquid phase change materials has been ignored. The fluid flow analysis in the studied problem (in each heating or cooling period) had two parts. One part contained only air (water) as a fluid, and the other part was a porous medium (combination of air and solid particles or water and solid particles). In the first part, the Navier–Stokes equations are used and in the second part, the Brinkman equation is used to describe the flow. The velocity field for the air region was calculated using Eq. (1) to Eq. (3). and for the porous region, using Eqs. (4) to Eq. (6) [26].

$$\rho\nabla.\mathbf{u} = 0 \quad (1)$$

$$\rho(\mathbf{u}.\nabla)\mathbf{u} = \nabla.[-p\mathbf{I} + \mathbf{K}] + \mathbf{F} + \rho\mathbf{g} \quad (2)$$

$$\mathbf{K} = (\mu + \mu_T)(\nabla\mathbf{u} + (\nabla\mathbf{u})^{\mathrm{T}}) \quad (3)$$

$$\frac{1}{\varepsilon_p}\rho(\mathbf{u}.\nabla)\mathbf{u}\frac{1}{\varepsilon_p} = \nabla.[-p\mathbf{I} + \mathbf{K}] - \left(\mu k^{-1} + \beta\rho|\mathbf{u}| + \frac{Q_m}{\varepsilon_p^2}\right)\mathbf{u} + \mathbf{F} + \rho\mathbf{g} \quad (4)$$

$$\rho\nabla.\mathbf{u} = Q_m \quad (5)$$

$$(\nabla.\mathbf{u})\mathbf{I}\mathbf{K} = \frac{1}{\varepsilon_p}(\nabla\mathbf{u} + (\nabla\mathbf{u})^{\mathrm{T}}) - \frac{2}{3}\frac{1}{\varepsilon_p} \quad (6)$$

According to the conditions of the problem, the flow field is considered turbulent in this problem. The standard κ-ε model has also been used to model turbulence. Eq. (7) and (8) show the governing relationships of this model for the air (water) region, and Eqs. (9) and Eq. Equation (10) shows the governing relationships of the porous region. The equation for the kinetic energy of turbulence K in the air region is as follows[26]:

$$\rho(\mathbf{u}.\nabla)k = \nabla.\left[\left(\mu + \frac{\mu_T}{\sigma_k}\right)\nabla\mathrm{k}\right] + p_k - \rho\varepsilon \quad (7)$$

The Diffusion rate equation ε for air (water) region is:

$$\rho(\mathrm{u}.\nabla)\epsilon = \nabla.\left[\left(\mu + \frac{\mu_T}{\sigma_\epsilon}\right)\nabla\epsilon\right] + c_{\epsilon 1}\frac{\epsilon}{k}p_k - c_{\epsilon 2}\rho\frac{\epsilon^2}{k}, \quad \epsilon = ep \quad (8)$$

The equation of the kinetic energy of turbulence K for the porous region is:

$$\rho(\mathbf{u}.\nabla)\frac{k}{\epsilon_p} = \nabla.\left[\left(\mu + \frac{\mu_T}{\sigma_k}\right)\nabla\mathrm{k}\right] + p_k + p_{k,porous} - \rho\varepsilon \quad (9)$$

The Diffusion rate equation ε for porous region is:

$$\rho(\mathbf{u}.\nabla)\frac{\epsilon}{\epsilon_p} = \nabla.\left[\left(\mu + \frac{\mu_T}{\sigma_\epsilon}\right)\nabla\epsilon\right] + c_{\epsilon 1}\frac{\epsilon}{k}p_k + p_{\epsilon,porous} - c_{\epsilon 2}\rho\frac{\epsilon^2}{k}, \quad \epsilon = ep \tag{10}$$

In the above equations, the values μ_T , p_k , $p_{k,porous}$ and $p_{\epsilon,porous}$ are calculated using Eqs. (11) to Eq. (15) [26].

$$\mu_T = \rho c_\mu \frac{k^2}{\epsilon\epsilon_p} \tag{11}$$

$$p_k = \frac{1}{\varepsilon_p}\mu_T[\nabla\mathbf{u}:(\nabla\mathbf{u})^T)] \tag{12}$$

$$p_{k,porous} = \rho\beta|\boldsymbol{u}|^3 \tag{13}$$

$$p_{\epsilon,porous} = C_{\epsilon 2}\frac{\rho C_{stpm}|\mathbf{u}|}{\mathrm{l}_{pore}\epsilon_p}\epsilon \tag{14}$$

$$\mathrm{l}_{pore} = \sqrt{k/\epsilon_p} \tag{15}$$

The problem studied from the perspective of energy is also divided into fluid and porous-medium parts. Equation (16) is the energy equation for the region that contains only air (water) and Eq. (18) to Eq. (24) represents the energy equation used for a porous medium[27].

$$\rho c_p\frac{\partial T}{\partial t} + \rho c_p\mathbf{u}.\nabla T + \nabla.\mathbf{q} = \mathrm{Q} + \mathrm{Q_{vd}} \tag{16}$$

$$,\mathrm{Q_{vd}} = \tau:\nabla\mathbf{u}$$

$$\mathbf{q} = -k\nabla T \tag{17}$$

$$\epsilon_p\rho_f c_{p,f}\frac{\partial T_f}{\partial t} + \rho_f c_{p,f}\boldsymbol{u}.\nabla T_f + \nabla.\mathbf{q}_f = Q_{s,f} + \epsilon_p Q_f + \epsilon_p Q_{vd} \tag{18}$$

$$\mathbf{q}_f = -\epsilon_p\, k_f\nabla T_f \tag{19}$$

$$\theta_s\rho_s c_{p,s}\frac{\partial T_s}{\partial t} + \nabla.\mathbf{q}_s = -Q_{s,f} + \theta_S Q_S \tag{20}$$

$$\mathbf{q}_\mathrm{s} = -\theta_s k_s\nabla T_s \tag{21}$$

$$Q_{s,f} = s_b h_{sf}(T_s - T_f) \tag{22}$$

$$s_b = \frac{6\theta_s}{d_{pe}} \tag{23}$$

$$h_{sf} = [d_{pe}(\frac{1}{k_f Nu} + \frac{1}{10k_s})]^{-1} \tag{24}$$

In Eq. (24), Nusselt number is obtained from Eq. (25) [28]:

$$Nu = 2.0 + 1.1pr^{1/3}Re_p^{0.6} \tag{25}$$

In addition, the particle Reynolds number and Parantel number were calculated using the following equations[26]:

$$Re_p = \frac{d_{pe}\rho_f\|\mathbf{u}\|}{\mu} \tag{26}$$

$$pr = \frac{\mu cp_f}{k_f} \tag{27}$$

The temperature distribution in the particles was computed using Eqs. 20, and phase-change function α. Therefore, the phase change occurs within the range of (Tm + ΔTm /2) to (Tm − ΔTm /2). When the temperature is less than (Tm-ΔTm/2), and greater than (Tm+ΔTm/2), the values of α are 0 and 1, respectively. During the phase change, the values of the conductive heat-transfer coefficient, density, and heat capacity change. These modifications are shown in Equations 28–32[26]:

$$\theta_1 = 1-\alpha \tag{28}$$

$$\rho = \theta_1\rho phase1 + (1-\theta_1)\rho phase2 \tag{29}$$

$$c_{p,s} = \frac{1}{\rho}(\theta_1\rho\mathrm{phase1}\ \mathrm{Cpphase1} + (1-\theta_1)\rho\mathrm{phase2Cpphase2}) + \mathrm{L}\frac{\partial\alpha_m}{\partial T} \tag{30}$$

$$\mathrm{K}_s = \theta_1\mathrm{Kphase1} + (1-\theta_1)\mathrm{Kphase2} \tag{31}$$

$$\alpha_m = \frac{(1-\theta_1)\rho phase2 - \theta_1\rho phase1}{2(\theta_1\rho\mathrm{phase1} + (1-\theta_1)\rho\mathrm{phase2})} \tag{32}$$

Using Eq. (1) to Eq. (32), the thermal performance of the model consisting of three types of phase change materials and the effects of the diameter, porosity, flow rate, and fluid temperature in two cooling and heating periods were investigated.

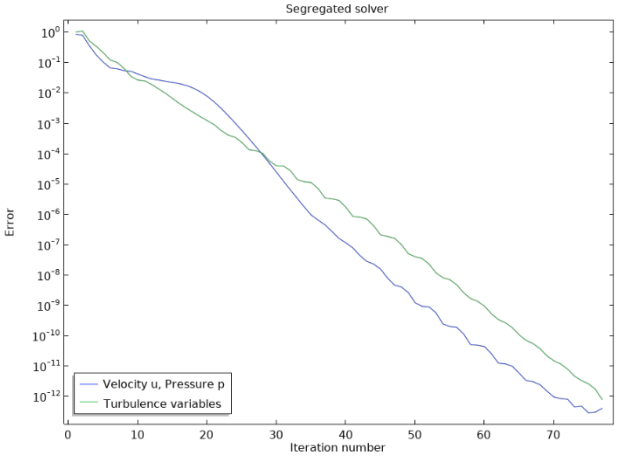

Fig .2. Convergence diagram of velocity, pressure, and turbulent flow variables for simulation.

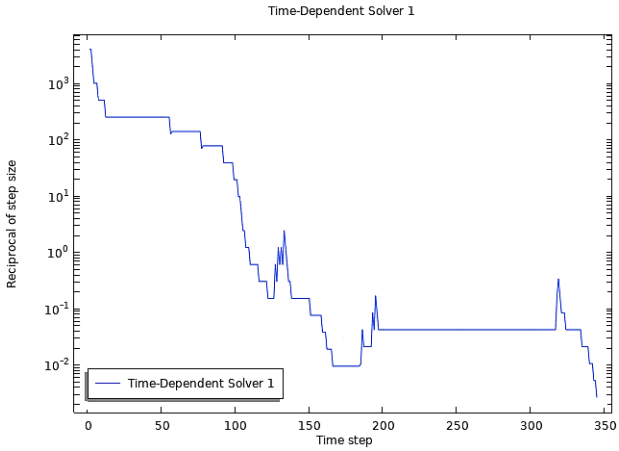

Fig.3. Convergence diagram of the non-steady state solution for the simulation

2.2. Boundary conditions

In this study, because the temperature of hot exhaust gases is in

the range of 100–160 °C [29]. A simulation was performed for this temperature range. In addition, the flow rate was considered variable in the range of 0.0025 to 0.01 m^3/s.

3. Results

3.1. Mesh independence study

To assess the independence of the numerical model from the computational grid and guarantee the minimal impact on the evaluated quantity with grid refinement, simulations of the heat exchanger using paraffin phase change material were conducted. The simulations considered a porosity of 0.49 and a particle diameter of 0.55 mm, employing three types of meshing. These meshes consisted of 5029, 7790, and 15502 elements, respectively, and the corresponding results are illustrated in Fig.4. Upon analysis, it was observed that the difference between modes 2 and 3 is negligible. Consequently, the second mode of the grid was adopted to reduce the computational expenses of the numerical modeling process. The grid used for the modeling is shown in Figure 5.

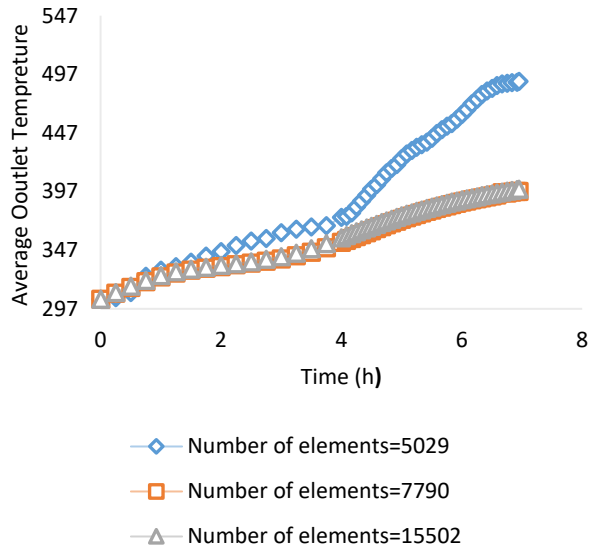

Fig.4. The average outlet temperature of the simulated model for different numbers of nodes was used to determine the mesh independence.

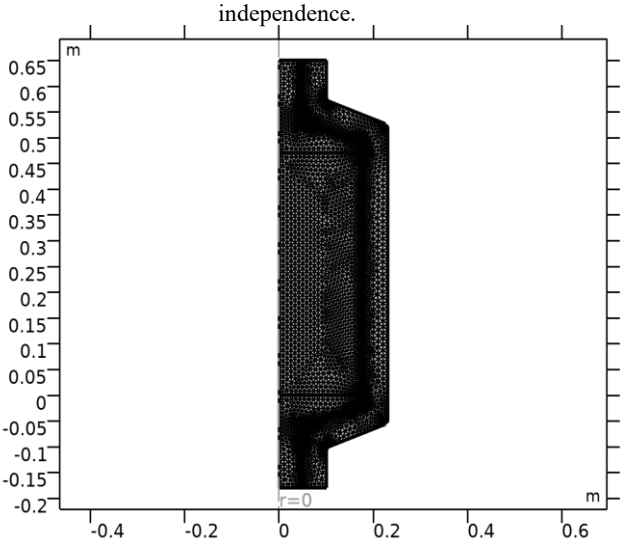

Fig.5. Mesh used for modeling in this study.

3.2. Validation

In order to validation of the study, the simulation consequences were compared with the experimental findings of the studies carried out by Barrientos et al [30]. Their experiment involved a fixed bed with phase change materials having a porosity of 0.468 and a median particle diameter of 1.64 mm, while air was used as the fluid. Figure 6 depicts the average temperature variations in both the simulated and experimental models over time. The results demonstrate suitable accuracy with a slight variance attributed to the absence of 100% insulation in the real scenario and the disparity in the displacement heat transfer coefficient between the simulation and real model.

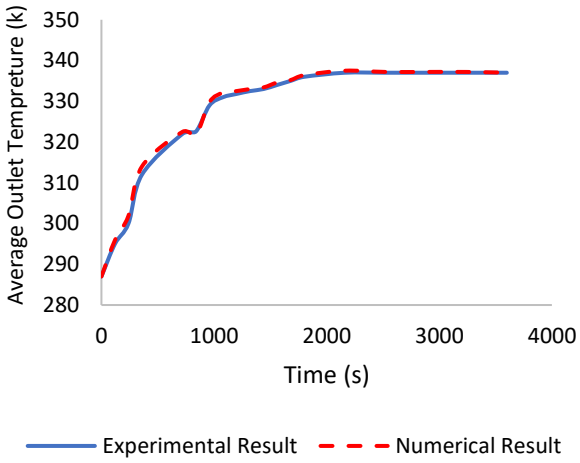

Fig.6. Average temperature changes in the simulated and experimental models versus time.

3.3. Simulation of the heating period

During this period, hot air with a temperature of 150 °C, a flow rate of 300 L/min, and other specifications listed in Table 2 enters the heat exchanger from the bottom, and after heat exchange with paraffin, its temperature decreases and from the top of the exchanger goes out. Figure 7 shows the changes in paraffin temperature, air temperature, and average temperature of the porous medium over time at the top (red), center (green), and bottom (blue) positions of the designed heat exchanger. As can be seen, initially due to the temperature difference between the inlet air and the system, the temperature increases in different positions of the exchanger until the temperature of the exchanger reaches about 60 degrees Celsius, which is the melting temperature of the phase change material (melting temperature of paraffin). At this time, in the porous area (where there is a phase change material), the phase change process begins and therefore there are no temperature changes, but after the complete melting of the paraffin and in other words the complete charging of the heat exchanger, the temperature increases again in different positions of the heat exchanger. Also, it is observed, during the phase change, the encapsulated paraffin was not in thermal equilibrium with the surrounding air. Measuring the air temperature at the inlet or outlet does not provide accurate information (neither the temperature inside the capsules nor the phase in which the paraffin wax is located).

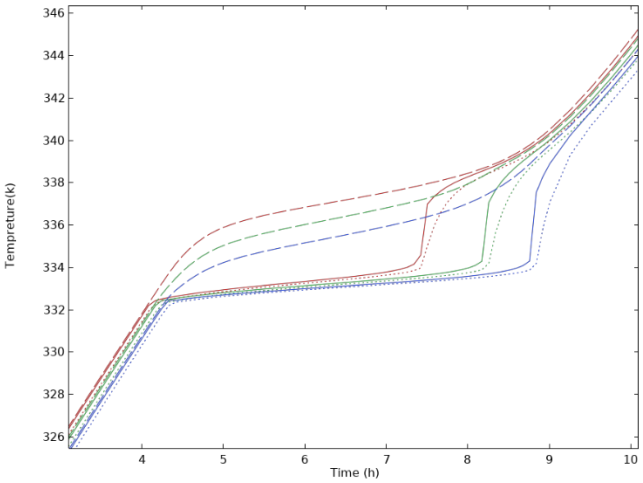

Fig.7. Diagram of temperature changes over time for air (dashed lin e), paraffin (dotted line), and the average porous medium (continuous li ne) at the top (red), center (green), and bottom (blue) positions of the st udied model.

Figure 8 shows the amount of paraffin melting over time in a heat exchanger with a porosity of 0.49 and a particle diameter of 0.55 mm during the heating period. As it can be seen, at the beginning, the paraffin is in the solid phase (Figure 8-a) and with the passage of time, the phase change process can be seen (Figure 8-b) and after 4 hours, a large part of the paraffin has melted. After 7 h (Figure 8-d), the paraffin material melted completely.

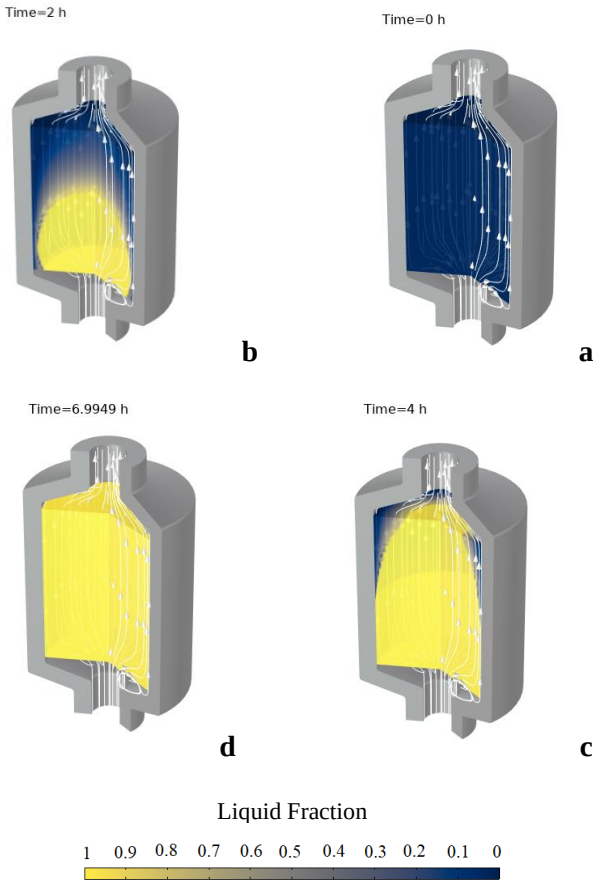

Fig.8. The phase changes over time-heating period.

3.4. Simulation of the cooling period

When melting of the paraffin was completed, in order to use the latent heating energy stored in the exchanger, cold water with a temperature of 20 ºc and a flow rate of 0.15 L/min enters the exchanger from the top. After exchanging heat with paraffin, the temperature increased and exited from the bottom of the exchanger. Figure 9 shows the freezing of paraffin over time in the simulation with a porosity of 0.49 and a particle diameter of 0.55 mm during the cooling period. As can be seen, at the beginning, the paraffin is in the liquid phase (Figure 9-a), and with the passage of time, the phase change process can be seen in Figure (9-b) and after 4 hours, a large part of the paraffin is frozen, and finally after 7 h (Figure 9-d), paraffin solidifies completely.

In the designed model, according to the difference in the type of fluid in the heating and cooling periods, the flow rate of the fluids in the two periods is determined in such a way that the process of charging and discharging occurs in almost equal times; thus, the proposed model can be used to recover energy from hot flue gases.

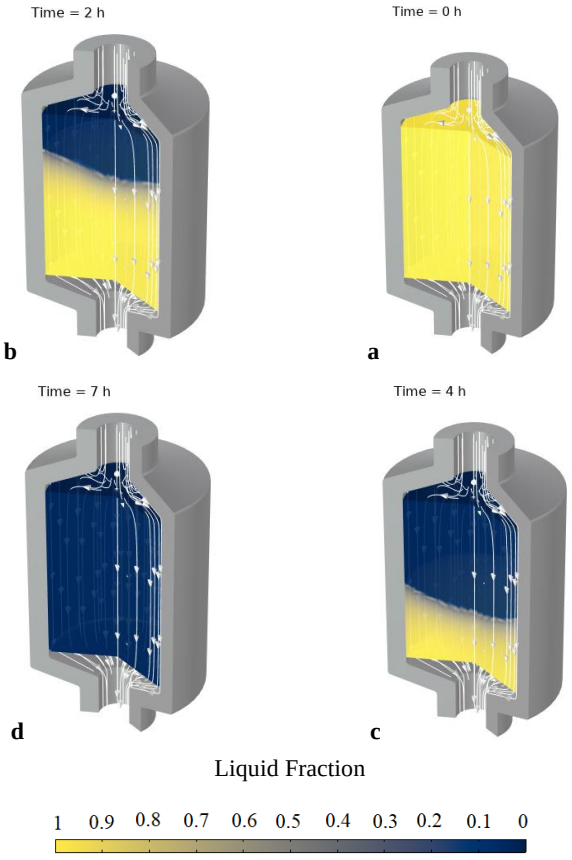

Fig.9. Phase changes over time-cooling period.

3.5. The effect of hot gases temperature

Among the important parameters in the performance of the proposed model is the inlet fluid temperature. In this research, according to the investigation, the temperature of the hot gases coming out of the chimney of steam boilers is in the range of 100 to 160 ºc [19]. The simulation has been done for the mentioned temperature range. Other parameters are also kept constant for comparison. Figure 10 shows the change of the average temperature of the porous area

over time for the heat exchanger with encapsulated particles with different inlet gas temperatures. As can be seen, with the increase in the temperature of the exhaust gases (inlet to the exchanger), the charging process of the exchanger takes place in a shorter time. According to the figure, it can be seen that at a temperature of 423.15 ° K, full charging takes place in about 7 hours, while for temperatures of 398.15 ° K and 383.15 ° K, the full charging time is about 9 and 11 hours, respectively.

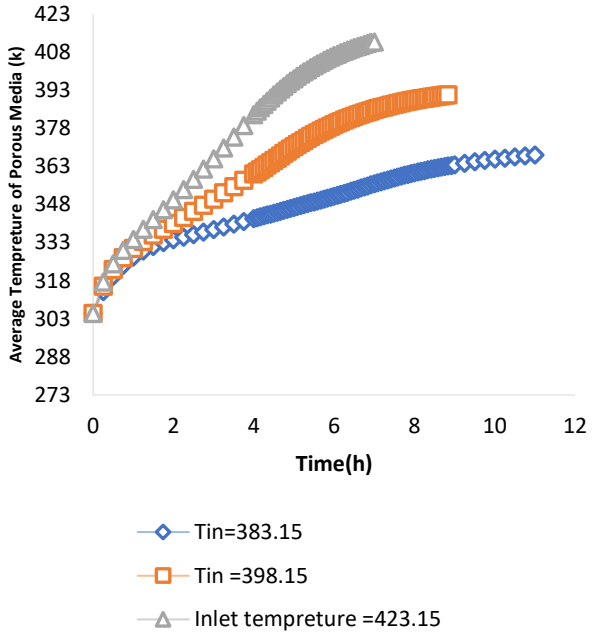

Fig.10. The average temperature changes of the designed heat exchanger over time for different temperatures of the hot gases exiting the chimney.

3.6. The effect of the Flow rate

Another important parameter is the hot fluid flow rate in the heating period, which according to the investigations carried out in different industries and different industrial equipment, the hot fluid flow rate ranges from 0.0025 to 0.01 m^3/s is considered. Other parameters are also kept constant for comparison. Figure 11 shows the average heat exchanger temperature changes over time for the heat exchanger with encapsulated particles in the heating period with different inlet gas flow rates. As can be seen, increasing the inlet fluid flow rate while other parameters are constant reduces the time for full charging of the heat exchanger. It can also be concluded that with the increase in velocity, the duration of fluid withdrawal with the desired temperature decreases. According to the figure, one can comprehend the significance of the suitable energy harvesting rate, a topic that has received relatively little discussion up to this point.

3.7. The effect of the Porosity

The amount of porosity is defined as the ratio of the volume occupied by air to the total volume of the phase change material and air during the heating period (or water during the cooling period). In this research, in order to investigate the effect of porosity on the thermal performance of the designed heat exchanger, the heat exchanger with three different geometries and porosity equal to 0.49, 0.20 and 0.8 and paraffin phase change material has been simulated. It should be noted that due to the constant volume of the chamber including phase change materials in all three simulated models and the definition of porosity, the volume and consequently the mass of solid particles are not the same and have the highest value in the state of 0.20 porosity. Figure 12 shows the average temperature changes of the designed heat exchanger over time for different porosities of the phase change material. As can be seen, with the decrease in porosity and as a result, the increase in the mass and quantity of the phase change material, the time required for the complete melting of the phase change material increases. As a result, the thermal energy stored by the heat exchanger increases.

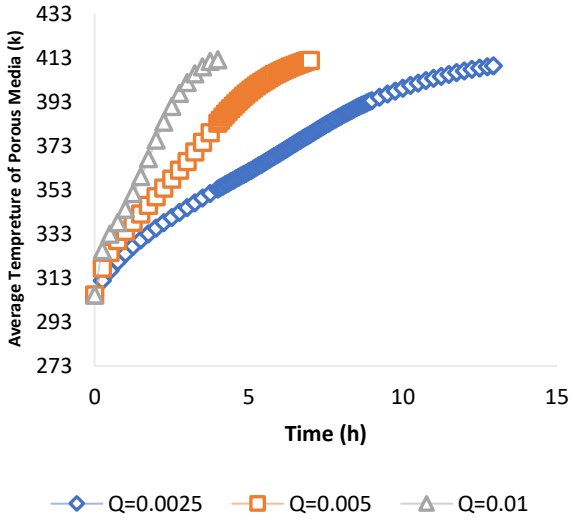

Fig.11. The average temperature changes of the designed heat exchanger over time for different flow rates of hot gases exiting the chimney.

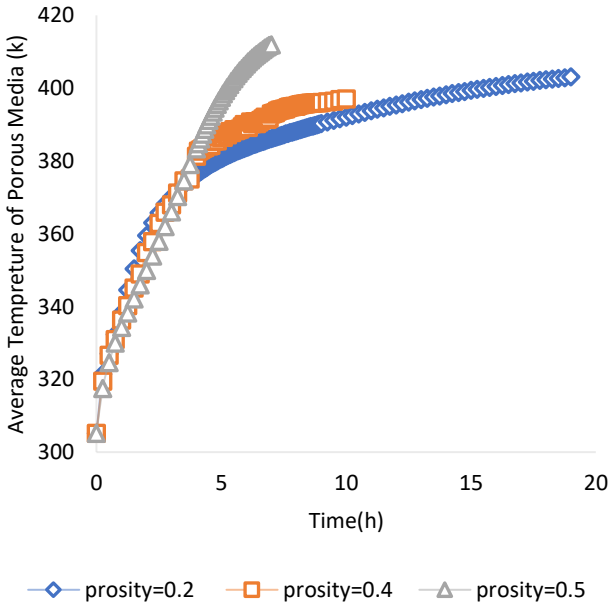

Fig.12. The average temperature changes of the designed heat exchanger versus time for different porosity of the phase change material.

3.8. The effect of the type of phase change material

The material phase change can occur in four ways: solid to solid,

solid to liquid, gas to solid, and gas to liquid. Among these, the solid to liquid phase change is applicable in heat exchangers due to technical limitations in other cases. There is a wide variety of phase change materials with different melting point ranges, classified into three groups: organic, inorganic, and eutectic. The selected PCMs in this paper are Paraffin, Potassium Fluoride Tetrahydrate, and Potassium Nitrate70% (KNO3-LINO3) that are organic, inorganic and eutectic phase change materials respectively. They were used to investigate their effect on the thermal performance of the designed heat exchanger. The details are presented in Table 2. Figure 13 depicts the average temperature changes of the heat exchanger over time for the three different materials. It is evident from the simulation models that all heat exchangers containing phase change materials were able to lower the average outlet temperature. However, over time, the temperature increased due to the melting of the phase change material. In addition, as can be seen from the Figure13, if potassium nitrate70% is used as a phase change material, the heat exchanger will be fully charged after approximately 24 hours, while in the case of paraffin and potassium fluoride tetrahydrate, the charging time will be about 7 hours and 5 hours respectively. Therefore, depending on the conditions of exhaust gases and energy consumption, each of these three materials can be used. Although paraffin is more practical in terms of availability and cost.

3.9. The effect of particle diameter

The performance of the newly designed heat exchanger is significantly dependent on the size of the particles. In this study, the particles' diameters were 10 mm, 55 mm, and 100 mm, and paraffin served as the phase change material. The volume of air remained constant compared to the total volume, and other factors were kept constant for a fair comparison (porosity is constant in three models). It is important to note that the mass of solid particles is consistent in all three models due to the constant volume and phase change material type. Figure 14 depicts the average temperature of the heat exchanger over time for the exchangers with different particle sizes. The graph indicates that as the particle diameter increases, the amount of time required for complete melting of the phase change material and the thermal energy stored by the heat exchanger increases.

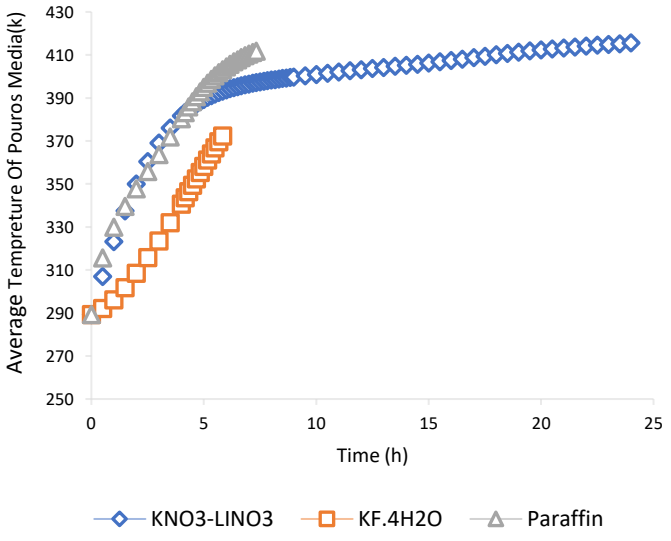

Fig.13. The average temperature changes of the designed heat exchanger versus time for three different types of phase change materials

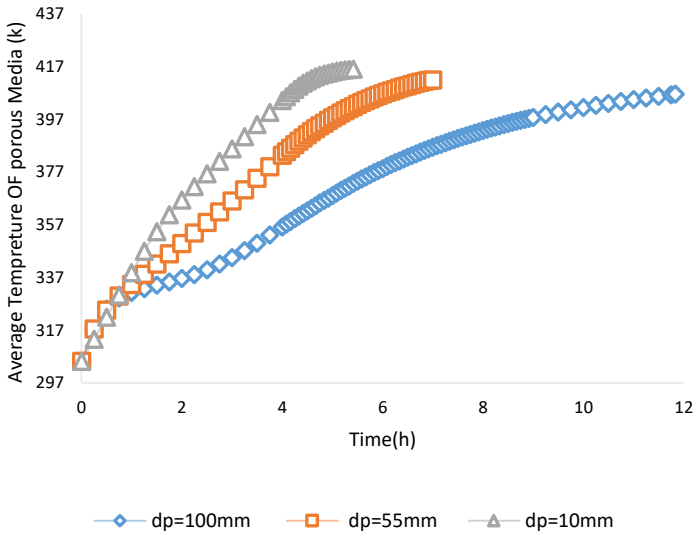

Fig.14. The average temperature changes of the designed heat exchanger versus time for three different particle diameters.

4. Conclusions

In the conducted investigation, a novel heat exchanger design incorporating encapsulated phase change materials has been replicated. The study portrays the heat exchanger as a homogeneous porous medium comprised of spherical capsules. Momentum and energy equations have been resolved based on the material science of the problem. The momentum equation was settled in a steady state, while the energy equation was handled in a non-steady state. To guarantee precise computations, a convergence accuracy of 10-12 was considered. The simulation, performed in three-dimensional mode, involved diverse geometries and three types of phase change material. The effect of several parameters, such as inlet fluid temperature, fluid flow rate, particle diameter, porosity, and type of phase change material on the thermal performance of the proposed system has been scrutinized. The results indicate a substantial reduction in the average temperature of the simulated heat exchanger compared to conventional exchangers, demonstrating an enhancement in thermal performance. Moreover, the findings reveal that decreasing porosity and increasing the diameter of solid particles boost the energy storage capacity and improve the exchanger's performance. Additionally, investigations into different inlet temperatures suggest that increasing the temperature of exhaust gases from the chimney enhances the heat exchanger's performance. Furthermore, varying flow rates show that increasing the inlet fluid flow rate, while maintaining other parameters constant, reduces the time required for the heat exchanger to reach full charge. Finally, the use of Kno3-Lino3 was found to increase the full charge time and the amount of stored energy compared to K.4h2o and paraffin, due to the improved properties and high melting temperature. Although paraffin is more practical in terms of availability and cost.

References

[1] R. Amirante, E. Cassone, E. Distaso, and P. Tamburrano, "Overview on recent developments in energy storage: Mechanical, electrochemical and hydrogen technologies, " Energy Convers Manag, vol.48, no.37, pp.372–87,2017.

[2] A. Gil, M. Medrano, I. Martorell, A. Lazaro, P. Dolado, B. Zalba, et al. "State of the art on high temperature thermal energy storage for power generation. Part 1econcepts, materials and modulization, " Renewable Sustainable Energy Rev, vol.14, no.1, pp.31-55,2010.

[3] D. Fernandes, F. Pitié, G. Cáceres, and J. Baeyens, "Thermal energy storage: "How previous findings determine current research priorities" ", *Energy*, vol.39, no.1, pp. 246-257,2012.

[4] M. Shahabi, H. A. Ozgoli, A.Akbarnia, "Modeling and Investigation of Gas Turbines Heat Recovery in the Semnan Oil Pumping Station for Heating Gas-Oil to Reduce Energy Consumption of Pumping, " *Journal of Energy Management and Technology*, vol.4, no.4, PP.21-27, 2020. doi: 10.22109/jemt.2020.211562.1214

[5] A. Sharma, V. Tyagi, C.R. Chen, and D. Buddhi, "Review on thermal energy storage with phase change materials and applications," *Renewable and Sustainable energy reviews*, vol.13, no.3, pp.18-345,2009.

[6] M. Sadrameli, in Transport Phenomena in Heat and Mass Transfer, 1992.

[7] A.F. Zobaa, Energy Storage: Technologies and Applications. BoD–Books on Demand, 2013.

[8] M. Šinka, D. Bajāre, A. Jakovičs, J. Ratnieks, S. Gendelis, J. Tihana, " Experimental testing of phase change materials in a warm-summer humid continental climate," *Energy and Buildings*, vol.195, no.1, pp.205-215,2019.

[9] M.Parwez, M. sefid, N. Perzai Khabazi, "Experimental investigation of the combined effect of condenser and phase change materials in the performance of single slope solar still," *Karafan Quarterly Scientific Journal*, vol.1,no.1,pp.1-10,2023. https://doi.org/10.48301/KSSA.2023.368106.2333

[10] M.Ebadati, A.Lork, M.H.Alizade Elizei, "The Effect of PCMs in the Building Shell on Energy Consumption Storage,"*Journal of Energy Management and Technology*, vol.7,no.2,pp.93-102,2023. doi: 10.22109/jemt.2022.309449.1336

[11] K. Pielichowska, and K. Pielichowski, "Phase change materials for thermal energy storage," *Progress in materials science*, vol.65, no.1, pp.14,67-123,2014.

[12] K. Oudaoui, M. Faraji, A. Benkaddour, M. Berra, "Numerical analysis of the thermal behavior of a solar heat exchanger using multiple phase change materials, "*Materials Today: Proceedings*,2024,https://doi.org/10.1016/j.matpr.2024.05.139.

[13] M. Rahimi, S. Ardahaie,M.J. Hosseini, and M. Gorzin, "Energy and exergy analysis of an experimentally examined latent heat thermal energy storage system, " *Renewable Energy*, vol.147,no.1,pp.1845-1860,2020.

[14] N.S.Roberts, R. Al-Shannaq, J. Kurdi, S. A., Al-Muhtaseb, and M.M. Farid, "Efficacy of using slurry of metal-coated microencapsulated PCM for cooling in a micro-channel heat exchanger, " *Applied Thermal Engineering*, vol.122, no.1, pp.11-18,2017.

[15] B. C., Zhao, and R. Z., Wang, "Perspectives for short-term thermal energy storage using salt hydrates for building heating. *Energy*, vol.189, no.1, pp.116139,2019.

[16] N. H. S., Tay, M., Liu, M., Belusko, and F., Bruno, "Review on transportable phase change material in thermal energy storage systems," *Renewable and Sustainable Energy Reviews*, vol.75, no.1, pp. 264-277,2017.

[17] J. M., Mahdi, and E. C., Nsofor, Solidification enhancement in a triplex-tube latent heat energy storage system using nanoparticles-metal foam combination. *Energy*, vol.126, no.1, pp. 501-512.2020.

[18] R., Karami, and B., Kamkari, "Investigation of the effect of inclination angle on the melting enhancement of phase change material in finned latent heat thermal storage units, "*Applied Thermal Engineering*, vol.146, no.1, pp. 45-60,2019.

[19] S. M., Borhani, M. J., Hosseini, A. A., Ranjbar, and R.,Bahrampoury, "Investigation of phase change in a spiral-fin heat exchanger, " *Applied Mathematical Modelling*, vol.67, no.1, pp. 297-314,2019.

[20] A. A., Al-Abidi, S., Mat, K., Sopian, M. Y., Sulaiman, and A. T. Mohammad, "Numerical study of PCM solidification in a triplex tube heat exchanger with internal and external fins," *International Journal of Heat and Mass Transfer*, vol.61, no.1, pp. 684-695,2013.

[21] N. H. S., Tay, M., Belusko, A., Castell, L. F., Cabeza, and F., Bruno, " An effectiveness-NTU technique for characterising a finned tubes PCM system using a CFD model, " *Applied energy*, vol. 131, no.1, pp.377-385,2014.

[22] A., Ebrahimi, M. J., Hosseini, A. A., Ranjbar, M., Rahimi, and R., Bahrampoury, "Melting process investigation of phase change materials in a shell and tube heat exchanger enhanced with heat pipe," *Renewable Energy*, vol. 138, no.1, pp. 378-394,2019.

[23] A., Haghighi, A., Babapoor, M., Azizi, Z., Javanshir, and H., Ghasemzade, "Optimization of the thermal performance of PCM nanocomposites," *Journal of Energy Management and Technology*, vol.4,no.2,pp.14-19,2020.

[24] P. J., Shamberger, and T., Reid, "Thermophysical Properties of Potassium Fluoride Tetrahydrate from (243 to 348), "*Journal of Chemical & Engineering Data*,vol.58,no.2,pp.294-300,2013.

[25] A., Dinker, M., adhu Agarwal, and G.D. Agarwal, " Heat storage materials, geometry and applications: A review, " *Journal of the Energy Institute*, vol. 90, no.1,pp. 1-11,2017.

[26] F.,Mohammadnejad, and S.Hossainpour, "A CFD modeling and investigation of a packed bed of high temperature phase change materials (PCMs) with different layer configurations" *Journal of Energy Storage*, vol.28,no.1,pp. 1-11.,2020. https://doi.org/10.1016/0009-2509(79)85064-2

[27] D.A Nield, and A., Bejan. Convection in Porous Media, in Convection Heat Transfer, (4nd ed.). *John Wiley & Sons*, Inc.2013. http://dx.doi.org/10.1007/978-1-4614-5541-7

[28] N., Wakao, S., Kaguei, and T.Funazkri, Effect of fluid dispersion coefficients on particle-to-fluid heat transfer coefficients in packed beds. Correlation of Nusselt numbers. Chemical Engineering Science,vol.34,no.3,pp.325-336.1979. https://10.1016/0009-2509(79)85064-2

[29] X., Zhai1, Sh., Tian, K., Zhu, P., Huang and J., Yu, and P., Huang, "Research on the experimental performance of gas-fired boiler based on the total heat recovery technology of absorption heat pump, "E3S Web of Conferences 261, 01059 ,2021.

[30] M, A., Izquierdo-Barrientos, C., Sobrino, J, A., Almendros-banez, "Thermal energy storage in a fluidized bed of PCM, " *Chem. Eng. J*. vol.230, no.1, pp.573–583,2013.